ARTICLE
Journal of Cellular Biochemistry 114:1584–1594 (2013)

Journal of Cellular Biochemistry

Increased Extracellular Matrix and Proangiogenic Factor Transcription in Endothelial Cells after Cocultivation with Primary Human Osteoblasts

F. Simunovic,[1] D. Steiner,[1] D. Pfeifer,[2] G.B. Stark,[1] Günter Finkenzeller,[1*] and F. Lampert[1]

[1]*Department of Plastic and Hand Surgery, Freiburg University Medical Center, Freiburg, Germany*

[2]*Department of Hematology and Oncology, Freiburg University Medical Center, Freiburg, Germany*

ABSTRACT

The most promising strategies in bone engineering have concentrated on providing sufficient vascularization to support the newly forming tissue. In this context, recent research in the field has focused on studying the complex interactions between bone forming and endothelial cells. Our previous work has demonstrated that direct contact cocultivation of human umbilical vein endothelial cells (HUVECs) with primary human osteoblasts (hOBs) induces the osteogenic phenotype and survival of hOBs. In order to investigate the mechanisms that lead to this effect, we performed microarray gene expression profiling on HUVECs following cocultivation with hOBs. Our data reveal profound transcriptomic changes that are dependent on direct cell contact between these cell populations. Pathway analysis using the MetaCore™ platform and literature research suggested a striking upregulation of transcripts related to extracellular matrix and cell-matrix interactions. Upregulation of a number of major angiogenetic factors confirms previous observations that HUVECs enter a proangiogenic state upon cocultivation with osteoblasts. Interestingly, the downregulated transcripts clustered predominantly around cell cycle-related processes. The microarray data were confirmed by quantitative real-time RT-PCR on selected genes. Taken together, this study provides a platform for further inquiries in complex interactions between endothelial cells and osteoblasts. J. Cell. Biochem. 114: 1584–1594, 2013.

KEY WORDS: BONE TISSUE ENGINEERING; EXTRACELLULAR MATRIX; ANGIOGENESIS; HUMAN UMBILICAL VEIN ENDOTHELIAL CELLS; GENE EXPRESSION PROFILING

Any three-dimensional (3D) tissue is dependent on sufficient supply with oxygen and nutrients. Therefore, apart from bradytrophic tissues such as cartilage, the formation of a vascular network by means of angiogenesis or vasculogenesis is a prerequisite for the development and regeneration of viable structures beyond the range of diffusion. It follows that understanding and gaining control of the angiogenic processes are pivotal issues in bone tissue engineering applications as well as in the clinical setting of fracture healing or bone regeneration [Kaully et al., 2009].

There is ample scientific literature dealing with the interaction between endothelial cells and cocultivated osteoblasts [reviews in Grellier et al., 2009a; Das and Botchwey, 2011]. The osteoinductive and proliferative effect on osteoblasts, as well as importance of different communication modalities in this interaction such as paracrine signaling or direct cell contacts has been extensively studied by us and others [Guenther et al., 1986; Decker et al., 1995; Stevens and Williams, 1999; Street et al., 2002; Villars et al., 2002; Carano and Filvaroff, 2003; Stahl et al., 2004; Finkenzeller et al., 2006, 2010; Guillotin et al., 2008; Hager et al., 2009].

The majority of these studies investigate the osteoinductive effect of human umbilical vein endothelial cells (HUVECs) on human osteoblasts (hOBs), whereas only a few [Unger et al., 2007; Hofmann et al., 2008] examine the effect of cocultivation on HUVECs. In order to fully appreciate the mechanisms that underlie this interaction, it is essential to examine both cell types. We have therefore recently

F. Simunovic and D. Steiner contributed equally to this work.

No competing financial interests exist.

Additional supporting information may be found in the online version of this article.

Grant sponsor: Deutsche Forschungsgemeinschaft (DFG); Grant number: FI 790/4-1.

*Correspondence to: Günter Finkenzeller, Ph.D., Department of Plastic and Hand Surgery, Freiburg University Medical Center, Hugstetterstr. 55, 79106 Freiburg, Germany. E-mail: guenter.finkenzeller@uniklinik-freiburg.de

Manuscript Received: 1 August 2012; Manuscript Accepted: 8 January 2013

Accepted manuscript online in Wiley Online Library (wileyonlinelibrary.com): 17 January 2013

DOI 10.1002/jcb.24500 • © 2013 Wiley Periodicals, Inc.

investigated proliferation and apoptosis rates in both cell types, and in different culturing conditions [Steiner et al., 2012].

In the present study, we performed gene expression profiling by oligonucleotide microarrays. Our results indicate that profound transcriptomic changes are induced in HUVECs by direct cocultivation with hOBs, but not by indirect cocultivation. The majority of the differentially expressed transcripts were upregulated and, interestingly, the transcripts clustered around functional categories such as extracellular matrix remodeling and angiogenesis. Another highly enriched category was cell cycle, and most of the genes belonging to this category were downregulated. This data may serve as a basis for further investigations into the interactions between bone forming and endothelial cells.

MATERIALS AND METHODS

CELL CULTURE

hOBs were isolated from fresh bone material with the informed consent from the patients undergoing hip replacement surgery according to hospital ethic committee guidelines. Isolation of hOBs from bone material was performed as previously described [Wenger et al., 2004]. hOBs were cultured in medium 199 with Earle's salt (GIBCO, Eggenstein, Germany), supplemented with 10% heat-inactivated FCS, 1% L-glutamine, and 1% penicillin/streptomycin at 37°C, 5% CO_2. HUVECs were purchased from Promocell (Heidelberg, Germany) and cultured in endothelial cell growth medium (ECGM) supplemented with 10% FCS at 37°C, 5% CO_2, in a humidified atmosphere. Only HUVECs from passage 2 to 5 were used for the experiments.

For direct coculture experiments, osteoblasts and HUVECs were mixed in a ratio of 1:1 (1×10^5 hOBs + 1×10^5 HUVECs), seeded in six-well cluster plates and cultivated in ECGM, 10% FCS at 37°C, 5% CO_2 for 48 h. In the HUVEC monoculture group, HUVECs were seeded at 2×10^5 cells per well in six-well cluster plates in the growth medium described above.

For coculture experiments preventing direct cell contact, osteoblasts (2×10^5 per well) were seeded in six-well companion plates (Falcon) whereas HUVECs (2×10^5) were seeded onto cell culture insert membranes (1 μm pore size, Falcon). Osteoblasts and HUVECs were subsequently cocultivated for 48 h in the same culture vessel preventing direct cell contact but permitting diffusion of soluble molecules. In the corresponding HUVEC monoculture group, HUVECs were seeded at 2×10^5 cells onto cell culture insert membranes in six-well companion plates in the absence of hOBs in the growth medium described above and incubated for 48 h.

IMMUNOMAGNETIC SEPARATION

In order to separate HUVECs from hOBs after direct cocultivation, an immunomagnetic separation system (Invitrogen Dynal AS, Invitrogen, Karlsruhe, Germany) was used. In brief, cells were detached from the culture dishes by trypsin/EDTA treatment. Enzymatic digestion was stopped by addition of 500 μl PBS, 5% FCS. Thereafter, cells were centrifuged (1,000 rpm, 5 min) at room temperature and washed once with PBS, 0.1% BSA. Cells were resuspended in 1 ml of PBS, 0.1% BSA, mixed with 25 μl of magnetic beads (Dynabeads, Invitrogen) coated with an anti-CD31 antibody and incubated on a rotator for 30 min at 4°C. The HUVECs binding to the CD31-coated Dynabeads were separated using a magnetic particle concentrator (Invitrogen Dynal AS, Invitrogen) and used for further experiments. HUVECs grown in monoculture were treated in the same way in order to prevent that putative gene expression differences due to the separation process may appear in the expression profiling experiments.

MICROARRAY ANALYSIS

Total RNA from biological triplicates was prepared using the RNeasy Mini Kit (Qiagen, Hilden, Germany) according to manufacturer's instructions. The quality of the RNA was established using the Agilent RNA 6000 Nano Kit (Agilent Technologies, Santa Clara, CA). Following manufacture's instructions, 1 μl RNA probe was transferred in each sample well of the RNA nano chip. Subsequent analysis was performed with Agilent 2100 bioanalyzer. Mean RIN of the samples used in the study was 9.79 ± 0.24.

Of total RNA, 500 ng was processed with the Ambion WT Expression kit (Ambion, Austin, TX) as described by the manufacturer. The resulting cDNAs were fragmented and then labeled using the Affymetrix Terminal Labeling kit. Labeled fragments were hybridized to Affymetrix WT Human Gene ST 1.0 arrays for 16 h at 45°C with 60 rpm in an Affymetrix Hybridization oven 645. After washing and staining, the arrays were scanned with the Affymetrix GeneChip Scanner 3000 7G. CEL-files were produced from the raw data with Affymetrix GeneChip Command Console Software Version 3.0.1.

We used the Genedata Expressionist software for further data analysis. CEL files were imported into the Refiner (Version 7.0) module of Expressionist where GC background subtraction was performed using antigenomic background probes. Subsequently, quantile normalization and probe summarization was performed using the Bioconductor RMA condensing algorithm as implemented in Refiner [Irizarry et al., 2003]. Further analysis was performed in the Analyst module (Version 7.0) of Genedata Expressionist. Pathway enrichment analysis was conducted using the MetaCore™ platform (http://www.genego.com/metacore.php, GeneGo, St. Joseph, MI).

STATISTICAL ANALYSIS

To identify differentially expressed genes between two groups, the unpaired Bayes T-test [CyberT; Baldi and Long, 2001] with the Bayes Confidence Estimate Value set to 10 and a window size of 101 genes was used as a plugin within Analyst. To estimate the false discovery rate (FDR), the Benjamini–Hochberg q-value was calculated [Benjamini, 1995]. We then used the "Effect size" activity of Analyst to calculate the Effect size score between the experimental groups. Only genes from the categories "main" and "unmapped" (see Affymetrix transcript annotation NA32) were included in the analysis, excluding control probes. We set our significance thresholds for the effect size to 1.5-fold, accepted an FDR of $q = 0.1\%$, and excluded the non-annotated genes.

QUANTITATIVE REAL-TIME RT-PCR

TaqMan RT-PCR was carried out as previously described [Medhurst et al., 2000]. Total RNA was prepared from biological triplicates using the RNeasy Mini Kit (Qiagen) according to manufacturer's instructions. Total RNA (0.5 μg) was treated with three units of deoxyribonuclease I (DNase I, Invitrogen) to digest genomic DNA contamination. Random-primed cDNA synthesis was performed using 0.5 μg of DNase I-treated total RNA and 50 units of AffinityScript reverse transcriptase according to the manufacturer's instructions (Stratagene, Agilent, Santa Clara, CA). TaqMan PCR assays were performed in 384-well optical plates on a LightCycler (Roche, Mannheim, Germany) using Absolute QPCR ROX Mix (Abgene, Hamburg, Germany) according to the manufacturer's instructions. Oligonucleotide primers and probes for human GAPDH (GADPH forward: 5′-TGGGCTACACTGAGCACCAG-3′; GAPDH reverse: 5′-CAGCGTCAAAGGTGGAGGAG-3′, GAPDH probe: 5′-FAM-TCTCCTCTGACTTCAACAGCGACACCC-TAMRA-3′) were designed using the Primer Express software (Applied Biosystems, Forster City, CA) according to company guidelines. Oligonucleotide primers and TaqMan probes for human TNC (cat. no.: Hs01115665_m1), COL1A1 (cat. no.: Hs00164004_m1), COL1A2 (cat. no.: Hs00164099_m1), EDNRA (cat. no.: Hs03988672_m1), SEMA3D (cat. no.: Hs00380877_m1), TNFSF18 (cat. no.: Hs00183225_m1), BMPR1A (cat. no.: Hs01034913_g1), POSTN (cat. no.: Hs00170815_m1), and CXCL11 (cat. no.: Hs04187682_g1) were purchased from Applied Biosystems. The thermal cycling conditions were 95°C for 15 min followed by 50 cycles at 95°C for 15 s and at 60°C for 1 min. Data were analyzed using the relative standard curve method, with each sample being normalized to GAPDH. Statistically significant differences between groups were determined by using an unpaired Student's *t*-test. Statistical significance was defined when $P < 0.05$.

RESULTS

Following direct or indirect cocultivation, HUVECS were separated from the osteoblasts. The RNA was isolated from the HUVECs and subjected to the microarray analysis comparing the expression profiles of the cocultured HUVEC samples with those of the monocultured HUVECs. Using the cyber *t*-test, we found 3,983 differentially expressed genes with FDR equal to or smaller than 10% in the direct coculture, and 576 in the transwell culture. When the cut-off was set at greater than 1.5-fold change, and after excluding the non-annotated hits, 460 genes were upregulated and 305 downregulated in the direct coculture conditions, whereas 23 genes were up- and 44 downregulated in the indirect culture conditions (Fig. 1; Supplementary Table S1). Among the 23 upregulated genes in the indirect coculture, 6 were also represented in the gene group upregulated by direct coculture. Among the downregulated genes, there were 15 genes represented in both, direct and indirect, cocultures. Genes represented in both groups are highlighted in bold in the Supplementary Table S1.

Not only the number of genes but also the extent of gene expression was profoundly affected by direct cell contact, so that 20 genes were upregulated more that 10-fold relative to the monocultured cells (several higher than 50-fold), whereas no genes reached a change of more than fourfold in the downregulated direct, or up- and downregulated transwell groups. Of 25 highest upregulated genes, 13 encode for components of the ECM (marked bold in Table I).

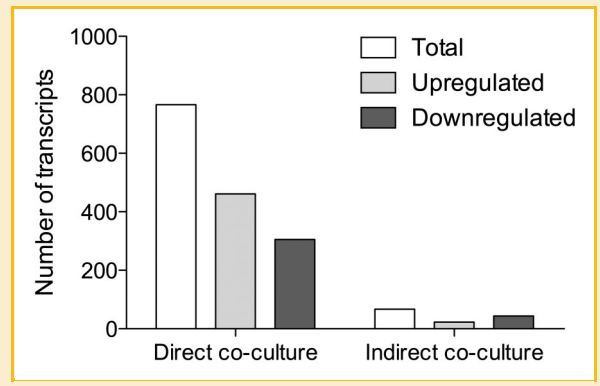

Fig. 1. Distribution of differentially expressed genes in HUVECs induced by direct or indirect co-culture with hOBs. Genes were derived by setting the cut-off at 1.5-fold, FDR at q = 0.1% and by excluding the non-annotated hits from the analysis (see Materials and Methods Section for details). Bars represent the numbers of transcripts in each group. Compared to the indirect coculture group, the expression of more genes was affected by direct cocultivation, and most of these were upregulated. Single genes can be found in the Supplementary Table S1, where genes represented in both, direct and indirect, cultures, are highlighted in bold.

After deriving the gene list, we asked whether the genes cluster around particular cellular functions. We approached this question from two different directions: firstly, by uploading our gene list into the MetaCore™ platform, we were able to extract the most significantly enriched pathways in our dataset (Fig. 2), and to examine the interactions between individual genes in those pathways. Secondly, we reviewed published literature on relevant cellular and tissue processes, after which we searched for the key players in our gene list. This approach enabled us to confirm the findings from pathway-level comparative computational analysis, but also to shed light on more complex phenomena which could have implications in bone tissue engineering, such as angiogenesis (Tables II–IV). We will discuss our findings according to most relevant functional categories derived by this combination of approaches.

EXTRACELLULAR MATRIX

A large number of upregulated genes, including some of the most upregulated genes in the whole dataset, such as decorin (DCN, 68.69-fold), tenascin C (TNC, 67.52-fold), collagen type VI, alpha 3 (COL6A3, 37.13-fold), proteoglycan 4 (PRG4, 46.93-fold), lumican (LUM, 47.04-fold), and matrix metallopeptidase 3 (MMP3, 22.62-fold) are important components of the ECM (Table II). Members of the integrin family and TNC are important in mechanotransduction of extracellular signals. Intriguingly, HUVECs also exhibited an upregulation of a number of growth factors which act through, or in synergy with the components of the ECM, such as vascular endothelial growth factor A (VEGFA, 1.9-fold), fibroblast growth

TABLE I. Genes Exhibiting Highest Up- or Down-Regulation in HUVECs Upon Direct Cocultivation With hOBs

Gene symbol	Description	Fold change	*P*-value
Upregulated genes			
DCN	**Decorin**	**68.69**	**1.00E−35**
TNC	**Tenascin C**	**67.52**	**1.00E−35**
CHI3L1	Chitinase 3-like 1 (cartilage glycoprotein-39)	54.31	1.00E−35
LUM	**Lumican**	**47.04**	**1.00E−35**
PRG4	**Proteoglycan 4**	**46.93**	**1.00E−35**
COL6A3	**Collagen, type VI, alpha 3**	**37.13**	**1.00E−35**
CRYAB	Crystallin, alpha B	35.13	1.00E−35
VCAN	**Versican**	**24.53**	**1.00E−35**
MMP3	**Matrix metallopeptidase 3 (stromelysin 1, progelatinase)**	**22.62**	**1.00E−35**
MFAP5	**Microfibrillar associated protein 5**	**19.24**	**1.00E−35**
WNT5A	Wingless-type MMTV integration site family, member 5A	18.61	1.00E−35
ENPP2	Ectonucleotide pyrophosphatase/phosphodiesterase 2	17.99	1.00E−35
SNAI2	Snail homolog 2 (Drosophila)	17.68	1.00E−35
SERPINA3	**Serpin peptidase inhibitor, clade A (alpha-1 antiproteinase, antitrypsin), member 3**	**15.85**	**2.22E−16**
COL1A2	**Collagen, type I, alpha 2**	**13.97**	**1.00E−35**
CP	Ceruloplasmin (ferroxidase)	12.81	2.00E−15
SULF1	Sulfatase 1	11.82	1.00E−35
CYP1B1	Cytochrome P450, family 1, subfamily B, polypeptide 1	11.07	1.00E−35
ISLR	Immunoglobulin superfamily containing leucine-rich repeat	10.92	1.55E−15
POSTN	Periostin, osteoblast-specific factor	10.55	1.00E−35
CMKLR1	Chemokine-like receptor 1	9.38	1.00E−35
COL3A1	**Collagen, type III, alpha 1**	**9.29**	**1.00E−35**
PLXDC2	Plexin domain containing 2	9.27	1.00E−35
COL1A1	**Collagen, type I, alpha 1**	**8.96**	**1.00E−35**
COL6A1	**Collagen, type VI, alpha 1**	**8.96**	**1.00E−35**
Downregulated genes			
SEMA3D	Sema domain, immunoglobulin domain (Ig), short basic domain, secreted (semaphorin), 3D	−3.85	2.00E−15
RNU5D	RNA, U5D small nuclear	−3.69	4.17E−09
TNFSF18	Tumor necrosis factor (ligand) superfamily, member 18	−3.69	2.01E−12
MEST	Mesoderm-specific transcript homolog (mouse)	−3.65	1.00E−35
RARB:LOC100130354	Hypothetical protein LOC100130354: retinoic acid receptor, beta	−3.41	1.31E−12
ADAMTS18	ADAM metallopeptidase with thrombospondin type 1 motif, 18	−3.33	1.78E−14
FOS	FBJ murine osteosarcoma viral oncogene homolog	−3.29	6.89E−12
LYPD1: GPR39	G protein-coupled receptor 39: LY6/PLAUR domain containing 1	−3.28	8.88E−16
C4orf49: NDUFC1	NADH dehydrogenase (ubiquinone) 1, subcomplex unknown, 1, 6 kDa: chromosome 4 open reading frame 49	−3.28	1.00E−35
C1orf110	Chromosome 1 open-reading frame 110	−3.01	5.44E−13
ZNF847P	Zinc finger protein 847, pseudogene	−2.96	6.97E−05
KRT7	Keratin 7	−2.89	1.00E−35
C21orf94	Chromosome 21 open-reading frame 94	−2.88	9.12E−07
WDR69	WD repeat domain 69	−2.82	4.74E−11
KCNAB1	Potassium voltage-gated channel, shaker-related subfamily, beta 1	−2.52	3.03E−13

Transcripts encoding for components of the ECM are shown in bold.

factor (FGF, 1.95-fold), transforming growth factor, beta (TGF-β, 2.69-fold) and bone morphogenetic protein receptor, type IA (BMPR1A, 5.35-fold). FGF, VEGF, EGF, as well as interleukins and Wnt family members (see below) bind to heparan sulfate (1.57-fold upregulated), a component of proteoglycans (PRG4, 46.93-fold upregulated). Additionally, a number of ECM components were described to play key roles in angiogenesis (marked bold in Table II).

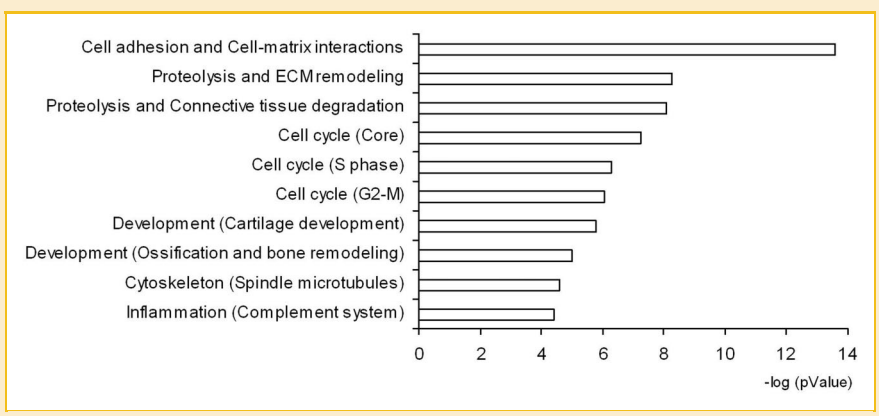

Fig. 2. Highest enriched cellular processes. Transcripts with altered expression in HUVECs by direct coculturing with hOBs were loaded into the MetaCore™ analysis software, and the processes ranked according to significance. Bars represent the inverse $\log_{10}$ of the *P* values.

TABLE II. Extracellular Matrix-Associated Transcripts

Gene symbol	Description	Fold change	*P*-value
A2M	Alpha-2-macroglobulin	6.86	1.00E−35
ACAN	Aggrecan	3.49	1.09E−08
ADAMTS2	ADAM metallopeptidase with thrombospondin type 1 motif, 2	4.71	1.17E−11
ADAMTS4	ADAM metallopeptidase with thrombospondin type 1 motif, 4	1.67	9.10E−08
ADAMTS5	ADAM metallopeptidase with thrombospondin type 1 motif, 5	1.69	0.0044
ADAMTS18	ADAM metallopeptidase with thrombospondin type 1 motif, 18	−3.33	7.40E−12
CD36	CD36 molecule (thrombospondin receptor)	1.84	1.09E−04
COL1A1	Collagen, type I, alpha 1	8.96	1.00E−35
COL1A2	Collagen, type I, alpha 2	13.97	1.00E−35
COL3A1	Collagen, type III, alpha 1	9.29	1.00E−35
COL6A1	Collagen, type VI, alpha 1	8.96	1.00E−35
COL6A2	Collagen, type VI, alpha 2	2.39	9.85E−10
COL6A3	Collagen, type VI, alpha 3	37.13	1.00E−35
COL12A1	Collagen, type XII, alpha 1	2.18	1.55E−09
COL14A1	Collagen, type XIV, alpha 1	1.91	9.37E−05
COL15A1	Collagen, type XV, alpha 1	1.71	0.0014
COMP	Cartilage oligomeric matrix protein	1.82	1.62E−04
CSPG4	Chondroitin sulfate proteoglycan 4	3.81	3.25E−07
CTHRC1	Collagen triple helix repeat containing 1	1.66	8.37E−06
CTSK	**Cathepsin K**	**1.59**	**8.35E−07**
CTSO	Cathepsin O	1.78	1.56E−06
DCN	Decorin	68.69	1.00E−35
ECM1	Extracellular matrix protein 1	1.59	3.64E−05
ECM2	Extracellular matrix protein 2, female organ and adipocyte specific	1.60	0.0045
FSD2	Fibronectin type III and SPRY domain containing 2	−1.60	0.0829
HAPLN1	Hyaluronan and proteoglycan link protein 1	6.70	3.04E−13
HAPLN3	Hyaluronan and proteoglycan link protein 3	1.56	8.10E−05
HAS2	Hyaluronan synthase 2	8.62	1.64E−13
HMMR	Hyaluronan-mediated motility receptor (RHAMM)	−1.51	2.92E−05
HS3ST3B1	Heparan sulfate (glucosamine) 3-O-sulfotransferase 3B1	1.57	0.0015
ITGA10	**Integrin, alpha 10**	**2.07**	**8.95E−08**
ITGA11	**Integrin, alpha 11**	**5.06**	**2.55E−12**
ITGB8	**Integrin, beta 8**	**−2.08**	**2.29E−07**
ITGBL1	**Integrin, beta-like 1 (with EGF-like repeat domains)**	**2.54**	**6.30E−09**
LAMA2	Laminin, alpha 2	1.76	8.28E−04
LAYN	Layilin	2.39	1.69E−06
LUM	Lumican	47.04	1.00E−35
MAP9	Microtubule-associated protein 9	1.93	0.0044
MFAP4	Microfibrillar-associated protein 4	1.53	0.0146
MFAP5	Microfibrillar associated protein 5	19.24	1.00E−35
MMP3	**Matrix metallopeptidase 3 (stromelysin 1, progelatinase)**	**22.62**	**1.00E−35**
MMP10	**Matrix metallopeptidase 10 (stromelysin 2)**	**1.71**	**2.92E−08**
MMP12	**Matrix metallopeptidase 12 (macrophage elastase)**	**1.78**	**0.0023**
NID2	Nidogen 2 (osteonidogen)	2.42	3.04E−11
PRG4	Proteoglycan 4	46.93	1.00E−35
SEMA5A	Semaphorin 5A	1.68	8.00E−04
SERPINA1	Serpin peptidase inhibitor, clade A (alpha-1 antiproteinase, antitrypsin), member 1	6.24	1.06E−11
SERPINA3	Serpin peptidase inhibitor, clade A (alpha-1 antiproteinase, antitrypsin), member 3	15.85	2.22E−16
SERPINE2	**Serpin peptidase inhibitor, clade E (nexin, plasminogen activator inhibitor type 1), member 2**	**4.77**	**1.00E−35**
SERPINF1	Serpin peptidase inhibitor, clade F (alpha-2 antiplasmin, pigment epithelium derived factor), member 1	3.89	1.34E−11
SERPING1	Serpin peptidase inhibitor, clade G (C1 inhibitor), member 1	2.56	9.66E−09
SGCD	Sarcoglycan, delta (35 kDa dystrophin-associated glycoprotein)	2.79	1.79E−07
TFPI2	Tissue factor pathway inhibitor 2	2.24	1.00E−35
THBS2	Thrombospondin 2	2.58	1.17E−07
TIMP1	TIMP metallopeptidase inhibitor 1	1.83	7.66E−13
TIMP3	TIMP metallopeptidase inhibitor 3	4.14	2.73E−11
TIMP4	TIMP metallopeptidase inhibitor 4	4.20	2.34E−11
TNC	**Tenascin C**	**67.52**	**1.00E−35**
VCAN	Versican	24.53	1.00E−35

Transcripts with known relevance in angiogenesis are marked in bold.

ANGIOGENESIS

By investigating the pertinent literature for major players in angiogenesis, we recovered a number of relevant transcripts in our dataset (Table III). Among the most interesting candidates are VEGF, an important stimulator of endothelial cell growth and migration (1.90-fold upregulation) and platelet-derived growth factor (PDGF), an important factor in recruiting mural cells around channels formed by endothelial cells. PDGFB and PDGFD were moderately upregulated in our dataset (1.51- and 1.50-fold, respectively) whereas the PDGF receptors PDGFR-α and PDGFR-β exhibited prominent upregulation (5.42- and 4.73-fold, respectively). BMPR1A, an osteoinductive growth factor receptor with importance in angiogenesis was strongly upregulated (5.35-fold), as were its family members transforming growth factor β3 (TGF-β3, 1.88-fold) and β1 (2.69). Angiopoietin-like 5 (ANGPTL5, 2.25-fold) was upregulated, as well as several members of the procadherin, semaphorine, and chemokine families.

It is known that endothelial cells produce components of the basal membrane, but also the proteases required for degradation of the surrounding ECM [Hynes, 2009], which presents the initial step of

TABLE III. Angiogenesis-Associated Transcripts

Gene symbol	Description	Fold change	*P*-value
ANGPTL5	Angiopoietin-like 5	2.25	7.96E−07
BMPR1A	Bone morphogenetic protein receptor, type IA	5.35	4.46E−14
CCL23	Chemokine (C–C motif) ligand 23	8.18	1.00E−35
CCL28	Chemokine (C–C motif) ligand 28	1.66	1.15E−04
CCRL1	Chemokine (C–C motif) receptor-like 1	−1.60	4.13E−06
CMKLR1	Chemokine-like receptor 1	9.38	1.00E−35
COX7A1	Cytochrome *c* oxidase subunit VIIa polypeptide 1 (muscle)	1.56	6.00E−05
CSF1	Colony stimulating factor 1 (macrophage)	1.68	7.91E−10
CTNNA1 LRRTM2	Catenin (cadherin-associated protein), alpha 1, 102 kDa: leucine rich repeat transmembrane neuronal 2	1.53	0.0062
CXCL1	Chemokine (C motif) ligand 1	1.60	0.0031
CXCL11	Chemokine (C–×–C motif) ligand 11	4.81	1.00E−35
CXCL12	Chemokine (C–×–C motif) ligand 12	2.00	1.42E−06
CXCL6	Chemokine (C–×–C motif) ligand 6 (granulocyte chemotactic protein 2)	1.75	2.30E−05
FGF7: KGFLP1	Fibroblast growth factor 7: keratinocyte growth factor-like protein 1	1.70	1.29E−04
FGF7: KGFLP2	Fibroblast growth factor 7: keratinocyte growth factor-like protein 2	1.73	2.95E−04
IGF2:INS: INS-IGF2	Insulin-like growth factor 2 (somatomedin A): INS-IGF2 read through transcript: insulin	1.75	7.80E−06
NTN4	Netrin 4	−1.59	7.10E−10
PCDH17	Protocadherin 17	2.58	1.39E−10
PCDH18	Protocadherin 18	3.36	1.79E−12
PCDHB14	Protocadherin beta 14	2.13	4.17E−09
PCDHB15	Protocadherin beta 15	1.99	4.96E−05
PCDHB2	Protocadherin beta 2	1.84	1.21E−06
PCDHB4	Protocadherin beta 4	2.02	6.47E−05
PCDHB5	Protocadherin beta 5	1.51	2.49E−05
PDGFB	Platelet-derived growth factor beta polypeptide	1.51	8.60E−08
PDGFD	Platelet-derived growth factor D	1.50	1.71E−05
PDGFRA	Platelet-derived growth factor receptor, alpha polypeptide	5.42	2.44E−14
PDGFRB	Platelet-derived growth factor receptor, beta polypeptide	4.73	7.11E−15
SEMA3C	Sema domain, immunoglobulin domain (Ig), short basic domain, secreted (semaphorin), 3C	2.93	2.65E−09
SEMA3D	Sema domain, immunoglobulin domain (Ig), short basic domain, secreted (semaphorin), 3D	−3.85	2.00E−15
SEMA5A	Sema domain, seven thrombospondin repeats (type 1 and type 1 like), transmembrane domain (TM) and short cytoplasmic domain (semaphorin), 5A	1.68	3.53E−05
SEMA7A	Semaphorin 7A, GPI membrane anchor	2.86	4.91E−11
TCTEX1D1	Tctex1 domain containing 1	1.66	8.15E−07
TGFB2	Transforming growth factor, beta 2	−1.87	3.39E−10
TGFB3	Transforming growth factor, beta 3	1.88	7.09E−08
TGFBI	Transforming growth factor, beta-induced, 68 kDa	2.69	1.00E−35
TIMP1	TIMP metallopeptidase inhibitor 1	1.83	1.33E−15
TIMP3	TIMP metallopeptidase inhibitor 3	4.14	7.97E−14
TIMP4	TIMP metallopeptidase inhibitor 4	4.20	6.76E−14
VEGFA	Vascular endothelial growth factor A	1.90	9.93E−09
WNT5A	Wingless-type MMTV integration site family, member 5A	18.61	1.00E−35

angiogenesis. In this context, ''Proteolysis,'' ''ECM remodeling,'' and ''Connective tissue degradation'' were the highest-enriched MetaCore™ terms in our dataset (Fig. 2). Furthermore, ECM proteins themselves can contain angiogenesis-promoting domains and these proteins were consistently and strongly upregulated: COL1A1 (8.96-fold), COL1A2 (13.97-fold in the microarray and 36.51-fold in the q real-time RT-PCR), COL3A1 (9.29-fold), COL6A3 (37.13-fold), COL15A1 (1.71-fold) and laminin, alpha 2 (LAMA2, 1.76). Fibronectin type III and SPRY domain containing 2 (FSD2) was downregulated 1.60-fold and TNC was the second highest upregulated gene in the array (67.52-fold) and in the qRT-PCR (3,071.73-fold). Further, we observed an upregulation of cathepsin K (CTSK, 1.59-fold, Table II), several integrin family members, matrix metallopeptidase family members and serpin peptidase inhibitor (SERPINE2, 4.77-fold), which were also implicated in angiogenesis. This data might support the notion that the ECM and angiogenesis are functionally and structurally intimately connected.

Several transcripts in our list have known angiogenesis inhibiting roles, such as TIMP metallopeptidase inhibitor (TIMP) 1, 3, and 4 (Table III) and plasminogen activator inhibitor type 1 (see Table II). However, a vast majority of angiogenesis-related transcripts in our dataset were inducers of angiogenesis, suggesting that the direct cocultivation of HUVECs with hOBs might have an angiogenesis-promoting effect.

OSTEOGENESIS AND CELL CYCLE

''Bone remodeling'' was among the highly enriched cell processes (Fig. 2) in our dataset. After examining the individual relevant genes (Table IV), we noticed a prominent upregulation of BMPR1A (5.35-fold), receptor for the bone morphogenic protein, an osteoinductive growth factor family. Three components of the Wnt pathway were also present: WNT1 inducible signaling pathway proteins (WISP) 1 and 3 were upregulated 1.63- and 1.85-fold, and WNT5A was present in the list of highest upregulated genes with 18.61-fold change. Periostin (POSTN), another promoter of osteoblast proliferation and survival, was also among the highest upregulated genes with 10.55-fold change. Upregulation of the TGF-β pathway was represented with TGF-β3 (1.88-fold) and TGF-β1 (2.69-fold).

Interestingly, among the 10 highest enriched cellular processes, 4 were related to cell cycle: ''Cell cycle core,'' ''S phase,'' ''G2-M phase,'' and ''spindle microtubules'' (Fig. 2). Almost all pertinent genes, notably adenylate cyclase-associated protein (CAP2, −1.53-fold), cyclins A1 (−2.47-fold) and B1 (−1.58), cell division cycle-associated genes, forkhead box M1 (FOXM1, −1.50), lamin B1

TABLE IV. Cell Cycle and Osteogenesis-Related Transcripts

Gene symbol	Description	Fold change	*P*-value
Cell cycle-related genes			
AURKA	Aurora kinase A	−1.63	6.62E−10
BUB1B: PAK6	p21 protein (Cdc42/Rac)-activated kinase 6: budding uninhibited by benzimidazoles 1 homolog beta (yeast)	−1.79	3.58E−10
CAP2	CAP, adenylate cyclase-associated protein, 2 (yeast)	−1.53	5.30E−06
CCDC15	Coiled-coil domain containing 15	−1.76	3.61E−04
CCNA1	Cyclin A1	−2.47	1.47E−11
CCNB1	Cyclin B1	−1.58	1.02E−09
CDC20	Cell division cycle 20 homolog (*S. cerevisiae*)	−1.53	4.79E−12
CDC25A	Cell division cycle 25 homolog A (*S. pombe*)	−1.57	3.82E−05
CDC45	Cell division cycle 45 homolog (*S. cerevisiae*)	−1.61	1.11E−09
CDC6	Cell division cycle 6 homolog (*S. cerevisiae*)	−1.81	1.11E−08
CDC7	Cell division cycle 7 homolog (*S. cerevisiae*)	−1.79	1.54E−05
CDCA2	Cell division cycle associated 2	−1.54	8.71E−08
CDCA3	Cell division cycle associated 3	−1.69	6.68E−08
CDCA8	Cell division cycle associated 8	−1.61	3.07E−09
CENPI	Centromere protein I	−1.76	3.20E−09
CHAF1B	Chromatin assembly factor 1, subunit B (p60)	−1.63	2.04E−07
CKS1B	CDC28 protein kinase regulatory subunit 1B	−1.52	1.80E−11
CLSPN	Claspin	−1.93	4.14E−09
E2F7	E2F transcription factor 7	−1.67	1.57E−10
E2F8	E2F transcription factor 8	−1.65	4.94E−08
ESPL1	Extra spindle pole bodies homolog 1 (*S. cerevisiae*)	−1.60	4.61E−06
ETS1	v-ets erythroblastosis virus E26 oncogene homolog 1 (avian)	−1.62	3.03E−12
ETS2	v-ets erythroblastosis virus E26 oncogene homolog 2 (avian)	−1.57	1.01E−11
FEN1	Flap structure-specific endonuclease 1	−1.50	1.83E−07
FOXM1	Forkhead box M1	−1.50	1.10E−09
GMNN	Geminin, DNA replication inhibitor	−1.52	6.11E−07
GTSE1	G-2 and S-phase expressed 1	−1.54	5.07E−07
LCORL: NCAPG	Non-SMC condensin I complex, subunit G: ligand-dependent nuclear receptor corepressor like	−1.60	1.43E−10
LMNB1	Lamin B1	−1.52	6.96E−06
MCM10	Minichromosome maintenance complex component 10	−1.58	7.72E−07
MCM2	Minichromosome maintenance complex component 2	−1.58	9.43E−06
MND1	Meiotic nuclear divisions 1 homolog (*S. cerevisiae*)	−1.54	0.0014
NCAPG2	Non-SMC condensin II complex, subunit G2	−1.58	2.41E−07
NEK2	NIMA (never in mitosis gene a)-related kinase 2	−1.54	4.46E−07
ORC1	Origin recognition complex, subunit 1	−1.59	1.41E−05
PDGFB	Platelet-derived growth factor beta polypeptide	1.51	8.60E−08
PDGFRA	Platelet-derived growth factor receptor, alpha polypeptide	5.42	2.44E−14
PDGFRB	Platelet-derived growth factor receptor, beta polypeptide	4.73	7.11E−15
PLK1	Polo-like kinase 1	−1.50	5.41E−11
POLE2	Polymerase (DNA directed), epsilon 2 (p59 subunit)	−1.62	7.22E−07
POLQ	Polymerase (DNA directed), theta	−1.51	9.16E−05
POLR3G	Polymerase (RNA) III (DNA directed) polypeptide G (32 kDa)	−1.51	3.55E−08
RBL1	Retinoblastoma-like 1 (p107)	−1.50	4.05E−06
NEK2	NIMA (never in mitosis gene a)-related kinase 2	−1.54	4.46E−07
Osteogenesis-related genes			
BMPR1A	Bone morphogenetic protein receptor, type IA	5.35	4.46E−14
WISP1	WNT1 inducible signaling pathway protein 1	1.63	5.79E−05
WISP3	WNT1 inducible signaling pathway protein 3	1.85	9.88E−04
WNT5A	Wingless-type MMTV integration site family, member 5A	18.61	1.00E−35
POSTN	Periostin, osteoblast-specific factor	10.55	1.00E−35
COL1A2	Collagen, type I, alpha 2	13.97	1.00E−35
COX7A1	Cytochrome *c* oxidase subunit VIIa polypeptide 1 (muscle)	1.56	6.00E−05
ACTA2	Actin, alpha 2, smooth muscle, aorta	2.12	1.68E−12

(LMNB1, −1.52), and retinoblastoma-like 1 (RBL1, −1.50) were downregulated (Table IV).

QUANTITATIVE REAL-TIME RT-PCR VALIDATION OF MICROARRAY DATA

In order to validate our findings from the microarrays, we performed quantitative real-time PCR (q real-time RT-PCR) experiments. We assayed seven upregulated genes: COL1A2, COL1A1, BMPR1A, endothelin receptor A (ENDRA), TNC, CXCL11, and POSTN, and two downregulated genes: TNSF18 and SEMA3D. The genes were chosen based on their presumed functional importance. The direction of differential expression (up- or down-regulation) was concordant with the microarray data. Figure 3 demonstrates the results of the q real-time RT-PCR experiments, and the Supplementary Table S2 shows the comparison of fold change values between the Affymetrix microarray and the TaqMan q real-time RT-PCR experiments.

DISCUSSION

Providing adequate vascularization to the engineered tissues remains a major hurdle in tissue engineering of the bone, and regenerative medicine in general. To this end, several strategies have been proposed with the goal of creating large viable bone implants [Kaully et al., 2009]. One of these strategies is to cocultivate and coimplant the essential cell types: osteoblasts and endothelial cells.

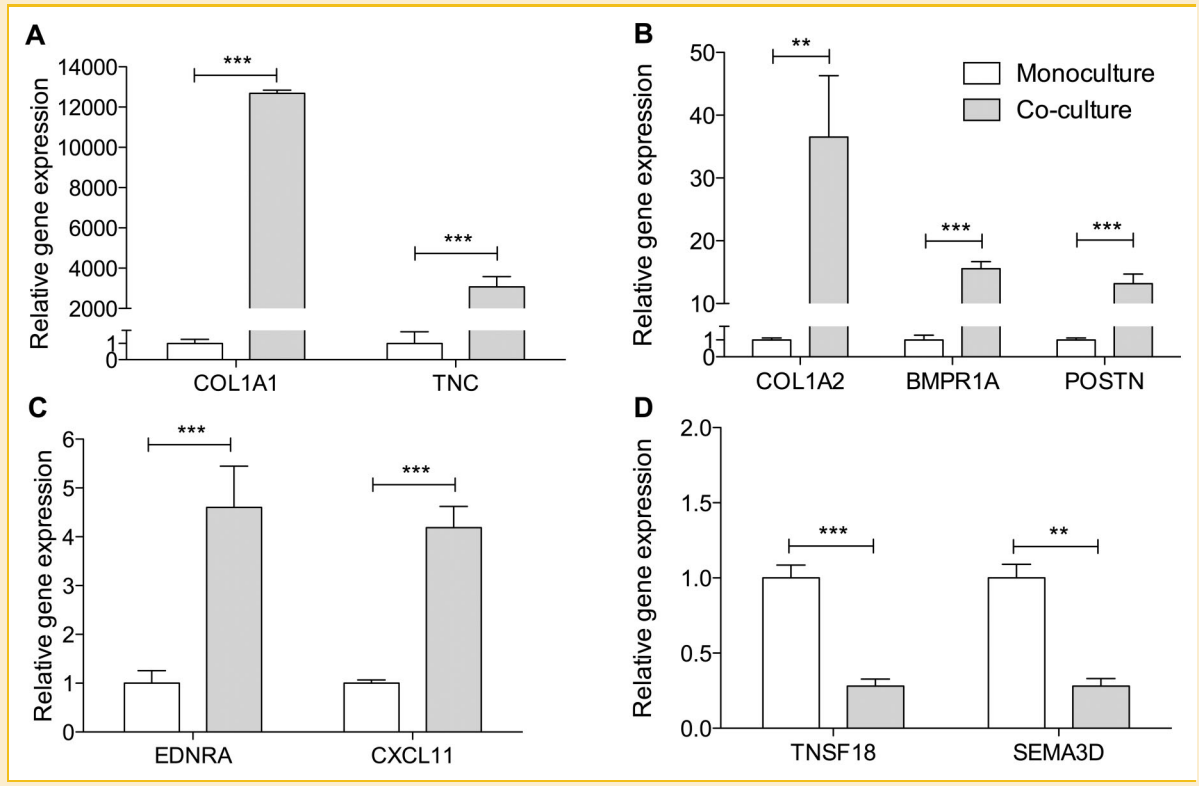

Fig. 3. TaqMan quantitative real-time RT-PCR validation of the microarray data. Relative gene expression in the HUVECs cocultured with hOBs was normalized to GAPDH and expressed relative to the monoculture conditions. Genes are shown as high (A), medium (B), low (C) upregulated, and downregulated (D) gene clusters. *P*-value < 0.0005 is indicated by three asterisks and $P < 0.005$ by two asterisks. Data present mean fold changes from three experiments.

It is known that osteogenesis, as well as angiogenesis, rely on complex cell-to-cell interactions [Nguyen and D'Amore, 2001]. Over the recent years we [Stahl et al., 2004; Finkenzeller et al., 2006; Hager et al., 2009; Finkenzeller et al., 2010], and others [Guenther et al., 1986; Wang et al., 1997; Villars et al., 2002; Sun et al., 2007; Guillotin et al., 2008; Grellier et al., 2009a], have shown that the interaction between hOBs and ECs is likely to be crucial for proper development of vascularized bone. For example, our group demonstrated that direct cell-to-cell contact causes an increase in transcript stability of the early osteoblastic marker alkaline phosphatase in osteoblasts [Hager et al., 2009] and others have confirmed this observation [Villars et al., 2002; Sun et al., 2007]. Furthermore, we recently demonstrated increased cell survival and anti-apoptotic effects on hOBs in the same cellular model [Steiner et al., 2012]. These findings suggest osteoinductive and anti-apoptotic effects following direct contact with HUVECs. However, the exact mechanisms of this interaction are not known.

Since it is known that also the HUVECs are modulated in their behavior by close proximity of hOBs [Hofmann et al., 2008], we attempted to gain insight into molecular mechanisms underlying this interaction by investigating the gene expression profile of HUVECs by Affymetrix microarrays. First, we asked whether the effect on HUVECs is mediated by soluble factors or by direct cell-to-cell communication. To answer this question, we cocultivated the cells in transwell chambers, preventing direct contact, and in direct 2D cultures. In accordance with our previous work in this experimental system, we observed extensive changes of gene expression upon 48 h of direct cocultivation, whereas physical separation of cells resulted in only minor changes. Only a minor number of genes were represented in both, direct and indirect cocultures, indicating that the changes that occur upon direct cocultivation are profoundly different from those induced by indirect cocultivation. Furthermore, the majority of the regulated transcripts were upregulated, and the upregulation reached striking fold changes, suggesting profound influence of hOBs on the HUVEC gene expression machinery.

INTERPLAY BETWEEN THE EXTRACELLULAR MATRIX AND ANGIOGENESIS

Intriguingly, the list of highly upregulated genes was enriched for transcripts related to extracellular matrix production, degradation and remodeling, which prompted us to run a MetaCore^{TM} pathway enrichment analysis, confirming this observation. The most significantly enriched pathway from this analysis, "Cell adhesion and Cell-matrix interactions," is visualized in Figure 4. It is known that the ECM serves an elaborate role in cellular physiology and pathology, serving not only as mechanical support for the cells but also by modulating cell morphology, migration, and differentiation [Hynes, 2009]. Its components can also directly influence cell signaling, either by directly transmitting mechanical extracellular signals into the cell and translating them into chemical signals (e.g., integrin and tyrosin kinase receptor signaling) [Hynes, 2002;

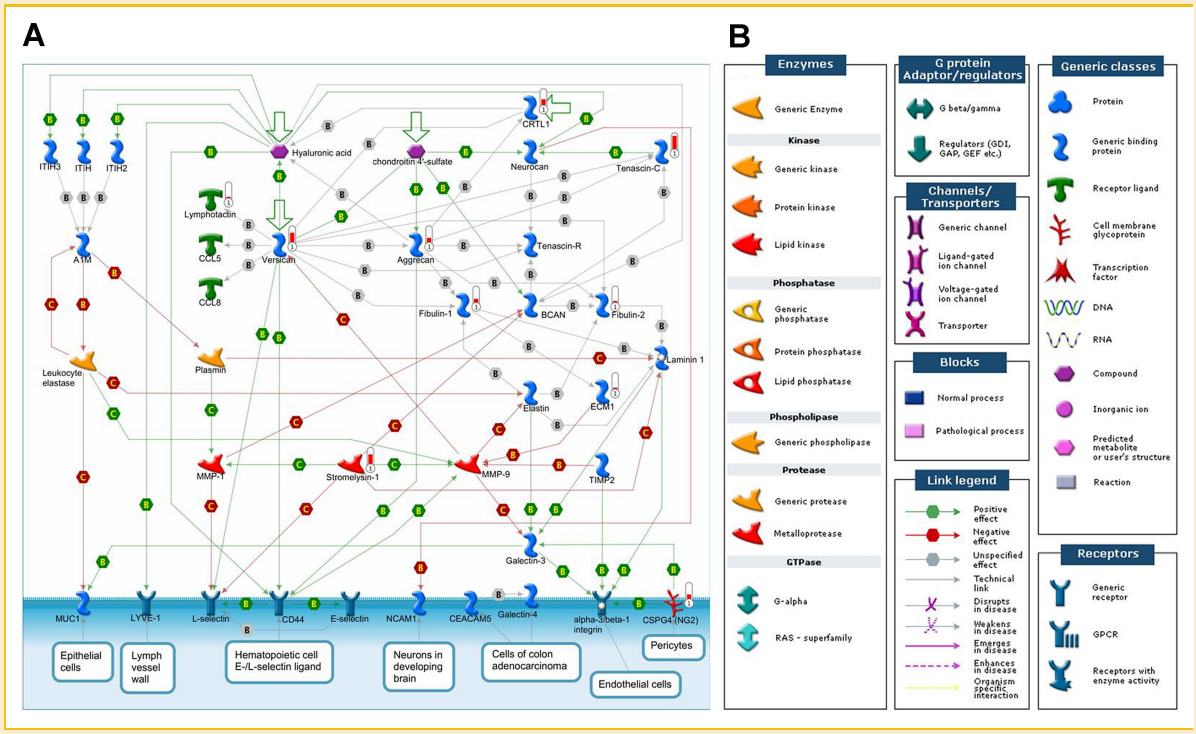

Fig. 4. Network of genes related to cell adhesion and extracellular matrix created with MetaCore™. Thermometers indicate that the transcripts were present in our dataset, and the red color indicates that the genes were upregulated. Green arrows labeled with "B" indicate binding, and red arrows labeled with "C" cleavage (A). Other symbols are explained in the figure legend (B).

Chiquet et al., 2009], or by binding soluble growth factors such as FGF, VEGF, TGF-β, and BMP [Hynes, 2009]. These growth factors, which were upregulated in our experiment, are then released by proteolysis or by mechanical strain and, in this fashion, the ECM controls their presentation to the cell. Furthermore, the ECM is structurally connected through the cytoskeletal network to the nucleus, allowing an uninhibited propagation of mechanical forces throughout the cell. This property is essential for development and maintenance of bone tissue [Zhang et al., 2012].

Recent work suggested an even more intimate relationship between the ECM and angiogenesis, suggesting that fragments of large ECM proteins may serve as direct stimulators or inhibitors of angiogenesis [Bix and Iozzo, 2005; Belotti et al., 2011]. These fragments have been termed "marticryptins," since they are often hidden and become exposed following conformational changes or proteolysis [Ricard-Blum and Ballut, 2011]. Most attention in this emerging field has been directed toward the use of ECM fragments for angiogenesis inhibition with the goal of controlling tumor growth and metastatic tumor spread [Bix and Iozzo, 2005; Noguera et al., 2012]. However, components of collagens I, III, IV and XV, laminin 1 and 8 [Kubota et al., 1988] and tenascin C [Hsia and Schwarzbauer, 2005] have been shown to posses proangiogenic effects on endothelial cells, mediated by integrin signaling. Several of these molecules and members of the integrin family were upregulated in our dataset.

Taken together, the transcriptional data presented in this study suggest that the balance between activators and inhibitors of angiogenesis is tipped in favor of activators and that the "angiogenic switch" [Carmeliet, 2005; Mundel and Kalluri, 2007] is turned on in endothelial cells upon cocultivation with hOBs. This finding is in accordance with previous work from our [Steffens et al., 2009] and other groups [Hofmann et al., 2008; Santos et al., 2009], which showed that HUVECs organize in tube-like structures with lumina when grown in 3D cocultures with hOBs.

OSTEOGENESIS

It has previously been shown that ECs have a direct osteoinductive activity in coculture with OBs, in addition to the supportive role as angiogenesis-driving cells [Grellier et al., 2009a, b], as measured by upregulation of early osteoblastic markers in hOBs following cocultivation. Interestingly, we have found prominent upregulation of genes related to osteogenesis, such as Wnt family members, TGF-β, BMPR1A, POSTN, and COL1.

Wnt, BMP, and TGF-β pathways are the paramount signaling pathways in osteogenesis [Gaur et al., 2005; Lian et al., 2006; Chen et al., 2012], several representatives of which are upregulated in our study. Another intriguing finding was the pronounced upregulation of periostin, an extracellular protein that has been implicated in osteoblast differentiation and survival, as well as ECM organization [Litvin et al., 2004; Zhu et al., 2009]. Interactions with tenascin C, bone morphogenic protein, collagen I, fibronectin, integrin family members and heparin have been described [Merle and Garnero, 2012], all of which were prominently upregulated in our dataset.

It is possible to speculate that the activation of these signaling pathways in ECs serves functions unrelated to osteogenesis, but important for EC function. For example, it is known that BMPs have an important role in angiogenesis [David et al., 2009], and that the Wnt signaling pathway has a broad influence on cell proliferation and differentiation [Klaus and Birchmeier, 2008].

CELL CYCLE

Whereas members of most enriched processes in our study were upregulated, we observed a consistent downregulation of genes linked to cell cycle-related processes. This is in line with our recent study, in which we observed that HUVEC-hOB cocultivation promotes the proliferation of hOBs, but not of HUVECs [Steiner et al., 2012]. Another group has cocultivated human dermal microvascular endothelial cells (HDMEC) with hOBs and could show increase in HDMEC survival. However, besides the fact that a different cell type was used, the model system was also different as the cells were cocultivated in 3D cultures on porous biomaterials [Unger et al., 2007]. Similarly, Hofmann et al. [2008] observed increased HUVEC proliferation and vessel-like structure formation in 3D cultures on polyurethane scaffolds after cocultivation with hOBs.

Taken together, these observations suggest that the proliferation of HUVECs is reduced in coculture with hOBs in our cellular model. As previously discussed, HUVECs are able to form capillary-like structures with lumen when cocultivated with hOB in 3D cultures. It seems possible that 3D culturing is necessary for HUVEC proliferation and subsequent capillary formation.

CONCLUSION

For the first time, we examined the transcription profile of HUVECs following cocultivation with hOBs. The data presented supports the notion that multifaceted interactions occur when bone-forming and blood vessel-forming cells are cultivated in direct contact. The role of ECs in OB differentiation appears to be far more complex than "mere" delivery of oxygen and nutrients via creation of new blood vessels. Our data support several observations from functional experiments on angiogenesis and osteogenesis in similar cellular models. Furthermore, this approach suggested the importance of ECM in this interaction. It also seems likely that the interplay between ECM components and angiogenic processes plays an important role.

It is, however, important to bear in mind that microarray data only represents a "snapshot" of the transcriptional network in one given moment [see Simunovic et al., 2009, 2010]. Although it is alluring to speculate about functional implications of the data, the data itself offer no information on protein levels or their function. Therefore, a microarray investigation can only serve as a starting point for further functional confirmation of the data. Nonetheless, when many members of particular groups of related genes cluster together around particular processes, as it is the case in this study, one can assume that these processes would be affected also on the protein level.

Another important question is that of cellular specificity. In the past, we have shown that single effects of hOB-HUVEC cocultivation, such as stabilization of osteoblastic ALP mRNA, are cell type specific [Hager et al., 2009]. However, we do not know whether changes such as reported in this study can be induced by other mesenchymal cell types, or perhaps even by cells derived from other lineages. As it is difficult to address this key question while conducting microarray experiments, cell specificity experiments will have to be early steps of any further study examining single aspects of this cellular interaction in more detail.

We have provided a platform for future inquiries into direct cell-to-cell communication between endothelial cells and primary hOBs. Research in this cellular model holds potential to deliver solutions that could improve vascularization of engineered bone constructs.

REFERENCES

Baldi P, Long AD. 2001. A Bayesian framework for the analysis of microarray expression data: regularized *t*-test and statistical inferences of gene changes. Bioinformatics 17:509–519.

Belotti D, Foglieni C, Resovi A, Giavazzi R, Taraboletti G. 2011. Targeting angiogenesis with compounds from the extracellular matrix. Int J Biochem Cell Biol 43:1674–1685.

Benjamini Y. 1995. Controlling the false discovery rate: a practical and powerful approach to multiple testing. J R Stat Soc Ser B (Methodol) 57:289–300.

Bix G, Iozzo RV. 2005. Matrix revolutions: "tails" of basement-membrane components with angiostatic functions. Trends Cell Biol 15:52–60.

Carano RA, Filvaroff EH. 2003. Angiogenesis and bone repair. Drug Discov Today 8:980–989.

Carmeliet P. 2005. Angiogenesis in life, disease and medicine. Nature 438:932–936.

Chen G, Deng C, Li YP. 2012. TGF-beta and BMP signaling in osteoblast differentiation and bone formation. Int J Biol Sci 8:272–288.

Chiquet M, Gelman L, Lutz R, Maier S. 2009. From mechanotransduction to extracellular matrix gene expression in fibroblasts. Biochim Biophys Acta 1793:911–920.

Das A, Botchwey E. 2011. Evaluation of angiogenesis and osteogenesis. Tissue Eng Part B Rev 17:403–414.

David L, Feige JJ, Bailly S. 2009. Emerging role of bone morphogenetic proteins in angiogenesis. Cytokine Growth Factor Rev 20:203–212.

Decker B, Bartels H, Decker S. 1995. Relationships between endothelial cells, pericytes, and osteoblasts during bone formation in the sheep femur following implantation of tricalciumphosphate-ceramic. Anat Rec 242:310–320.

Finkenzeller G, Arabatzis G, Geyer M, Wenger A, Bannasch H, Stark GB. 2006. Gene expression profiling reveals platelet-derived growth factor receptor alpha as a target of cell contact-dependent gene regulation in an endothelial cell-osteoblast co-culture model. Tissue Eng 12:2889–2903.

Finkenzeller G, Mehlhorn AT, Schmal H, Stark GB. 2010. Post-transcriptional regulation of osteoblastic platelet-derived growth factor receptor-alpha expression by co-cultured primary endothelial cells. Cells Tissues Organs 192:28–38.

Gaur T, Lengner CJ, Hovhannisyan H, Bhat RA, Bodine PV, Komm BS, Javed A, van Wijnen AJ, Stein JL, Stein GS, Lian JB. 2005. Canonical WNT signaling promotes osteogenesis by directly stimulating Runx2 gene expression. J Biol Chem 280:33132–33140.

Grellier M, Bordenave L, Amedee J. 2009a. Cell-to-cell communication between osteogenic and endothelial lineages: implications for tissue engineering. Trends Biotechnol 27:562–571.

Grellier M, Granja PL, Fricain JC, Bidarra SJ, Renard M, Bareille R, Bourget C, Amedee J, Barbosa MA. 2009b. The effect of the co-immobilization of human osteoprogenitors and endothelial cells within alginate microspheres on mineralization in a bone defect. Biomaterials 30:3271–3278.

Guenther HL, Fleisch H, Sorgente N. 1986. Endothelial cells in culture synthesize a potent bone cell active mitogen. Endocrinology 119:193–201.

Guillotin B, Bareille R, Bourget C, Bordenave L, Amedee J. 2008. Interaction between human umbilical vein endothelial cells and human osteoprogenitors triggers pleiotropic effect that may support osteoblastic function. Bone 42:1080–1091.

Hager S, Lampert FM, Orimo H, Stark GB, Finkenzeller G. 2009. Up-regulation of alkaline phosphatase expression in human primary osteoblasts by cocultivation with primary endothelial cells is mediated by p38 mitogen-activated protein kinase-dependent mRNA stabilization. Tissue Eng Part A 15:3437–3447.

Hofmann A, Ritz U, Verrier S, Eglin D, Alini M, Fuchs S, Kirkpatrick CJ, Rommens PM. 2008. The effect of human osteoblasts on proliferation and neo-vessel formation of human umbilical vein endothelial cells in a long-term 3D co-culture on polyurethane scaffolds. Biomaterials 29:4217–4226.

Hsia HC, Schwarzbauer JE. 2005. Meet the tenascins: multifunctional and mysterious. J Biol Chem 280:26641–26644.

Hynes RO. 2002. Integrins: bidirectional, allosteric signaling machines. Cell 110:673–687.

Hynes RO. 2009. The extracellular matrix: not just pretty fibrils. Science 326:1216–1219.

Irizarry RA, Hobbs B, Collin F, Beazer-Barclay YD, Antonellis KJ, Scherf U, Speed TP. 2003. Exploration, normalization, and summaries of high density oligonucleotide array probe level data. Biostatistics 4:249–264.

Kaully T, Kaufman-Francis K, Lesman A, Levenberg S. 2009. Vascularization—the conduit to viable engineered tissues. Tissue Eng Part B Rev 15:159–169.

Klaus A, Birchmeier W. 2008. Wnt signalling and its impact on development and cancer. Nat Rev Cancer 8:387–398.

Kubota Y, Kleinman HK, Martin GR, Lawley TJ. 1988. Role of laminin and basement membrane in the morphological differentiation of human endothelial cells into capillary-like structures. J Cell Biol 107:1589–1598.

Lian JB, Stein GS, Javed A, van Wijnen AJ, Stein JL, Montecino M, Hassan MQ, Gaur T, Lengner CJ, Young DW. 2006. Networks and hubs for the transcriptional control of osteoblastogenesis. Rev Endocr Metab Disord 7: 1–16.

Litvin J, Selim AH, Montgomery MO, Lehmann K, Rico MC, Devlin H, Bednarik DP, Safadi FF. 2004. Expression and function of periostin-isoforms in bone. J Cell Biochem 92:1044–1061.

Medhurst AD, Harrison DC, Read SJ, Campbell CA, Robbins MJ, Pangalos MN. 2000. The use of TaqMan RT-PCR assays for semiquantitative analysis of gene expression in CNS tissues and disease models. J Neurosci Methods 98: 9–20.

Merle B, Garnero P. 2012. The multiple facets of periostin in bone metabolism. Osteoporos Int 23:1199–1212.

Mundel TM, Kalluri R. 2007. Type IV collagen-derived angiogenesis inhibitors. Microvasc Res 74:85–89.

Nguyen LL, D'Amore PA. 2001. Cellular interactions in vascular growth and differentiation. Int Rev Cytol 204:1–48.

Noguera R, Nieto OA, Tadeo I, Farinas F, Alvaro T. 2012. Extracellular matrix, biotensegrity and tumor microenvironment. An update and overview. Histol Histopathol 27:693–705.

Ricard-Blum S, Ballut L. 2011. Matricryptins derived from collagens and proteoglycans. Front Biosci 16:674–697.

Santos MI, Unger RE, Sousa RA, Reis RL, Kirkpatrick CJ. 2009. Crosstalk between osteoblasts and endothelial cells co-cultured on a polycaprolactone-starch scaffold and the in vitro development of vascularization. Biomaterials 30:4407–4415.

Simunovic F, Yi M, Wang Y, Macey L, Brown LT, Krichevsky AM, Andersen SL, Stephens RM, Benes FM, Sonntag KC. 2009. Gene expression profiling of substantia nigra dopamine neurons: further insights into Parkinson's disease pathology. Brain 132:1795–1809.

Simunovic F, Yi M, Wang Y, Stephens R, Sonntag KC. 2010. Evidence for gender-specific transcriptional profiles of nigral dopamine neurons in Parkinson disease. PLoS ONE 5:e8856.

Stahl A, Wenger A, Weber H, Stark GB, Augustin HG, Finkenzeller G. 2004. Bi-directional cell contact-dependent regulation of gene expression between endothelial cells and osteoblasts in a three-dimensional spheroidal coculture model. Biochem Biophys Res Commun 322:684–692.

Steffens L, Wenger A, Stark GB, Finkenzeller G. 2009. In vivo engineering of a human vasculature for bone tissue engineering applications. J Cell Mol Med 13:3380–3386.

Steiner D, Lampert F, Stark GB, Finkenzeller G. 2012. Effects of endothelial cells on proliferation and survival of human mesenchymal stem cells and primary osteoblasts. J Orthop Res 10:1682–1689.

Stevens DA, Williams GR. 1999. Hormone regulation of chondrocyte differentiation and endochondral bone formation. Mol Cell Endocrinol 151:195–204.

Street J, Bao M, deGuzman L, Bunting S, Peale FV, Jr., Ferrara N, Steinmetz H, Hoeffel J, Cleland JL, Daugherty A, van Bruggen N, Redmond HP, Carano RA, Filvaroff EH. 2002. Vascular endothelial growth factor stimulates bone repair by promoting angiogenesis and bone turnover. Proc Natl Acad Sci USA 99:9656–9661.

Sun H, Qu Z, Guo Y, Zang G, Yang B. 2007. In vitro and in vivo effects of rat kidney vascular endothelial cells on osteogenesis of rat bone marrow mesenchymal stem cells growing on polylactide-glycoli acid (PLGA) scaffolds. Biomed Eng Online 6:41.

Unger RE, Sartoris A, Peters K, Motta A, Migliaresi C, Kunkel M, Bulnheim U, Rychly J, Kirkpatrick CJ. 2007. Tissue-like self-assembly in cocultures of endothelial cells and osteoblasts and the formation of microcapillary-like structures on three-dimensional porous biomaterials. Biomaterials 28:3965–3976.

Villars F, Guillotin B, Amedee T, Dutoya S, Bordenave L, Bareille R, Amedee J. 2002. Effect of HUVEC on human osteoprogenitor cell differentiation needs heterotypic gap junction communication. Am J Physiol Cell Physiol 282: C775–C785.

Wang DS, Miura M, Demura H, Sato K. 1997. Anabolic effects of 1,25-dihydroxyvitamin D3 on osteoblasts are enhanced by vascular endothelial growth factor produced by osteoblasts and by growth factors produced by endothelial cells. Endocrinology 138:2953–2962.

Wenger A, Stahl A, Weber H, Finkenzeller G, Augustin HG, Stark GB, Kneser U. 2004. Modulation of in vitro angiogenesis in a three-dimensional spheroidal coculture model for bone tissue engineering. Tissue Eng 10:1536–1547.

Zhang P, Wu Y, Jiang Z, Jiang L, Fang B. 2012. Osteogenic response of mesenchymal stem cells to continuous mechanical strain is dependent on ERK1/2-Runx2 signaling. Int J Mol Med 29:1083–1089.

Zhu S, Barbe MF, Liu C, Hadjiargyrou M, Popoff SN, Rani S, Safadi FF, Litvin J. 2009. Periostin-like-factor in osteogenesis. J Cell Physiol 218:584–592.